The Research of Medical Science Review
ISSN: 3007-1208 & 3007-1216 Volume 3, Issue 10, 2025

COMPARATIVE ASSESSMENT OF CHEST X-RAY (CXR) WITH HRCT IN THE DETECTION OF PULMONARY TUBERCULOSIS

Sadia Malik [*1], Dr. Farooque Ahmed Haidari[2], Iqra Naz[3], Ayesha Bibi[4], Afshan Shahzadi[5], Aqsa Shahzadi[6], Zainab Fatima[7], Robaisha Urooj[8]

[*1,5,6,7,8]*Department of Physics, Government Sadiq College Women University (GSCWU), Bahawalpur, Pakistan*
[2]*Radiology Department, Bahawal Victoria Hospital (BVH), Bahawalpur, Pakistan*
[3,4]*Department of Physics, University of Lahore, Pakistan*

[*1]sadia.malik@gscwu.edu.pk
[*1]https://orcid.org/0009-0002-2319-4373

DOI: https://doi.org/10.5281/zenodo.17935216

Keywords
Tuberculosis, Dose rate, Computed Tomography, High Resolution Computed Tomography

Article History
Received: 11 July 2025
Accepted: 21 September 2025
Published: 06 October 2025

Copyright @Author
Corresponding Author: *
Sadia Malik

Abstract

The main objective of this study is to compare the plane chest x-ray with HRCT in the pursue of the diagnosis and treatment of pulmonary tuberculosis. Pakistan is one of the eight nations that accounts for two-thirds of all new cases of developing TB. The standard clinical presentation features make it difficult for healthcare personnel to effectively evaluate the illness and prevent the spread of these fatal diseases. To counteract the sudden increase in TB cases, appropriate management and effective policies must be implemented. Thus, in order to prevent the spread of these infectious diseases, it is critical to recognise and address the problems that the healthcare sector faces, as well as to create an atmosphere in which the healthcare sector can function at its full potential.

Historically, plain chest X-rays have provided sufficient information for TB assessment, however, with advancements in imaging technology, HRCT is now considered more sensitive due to its higher resolution and superior image quality. This study aims to compare the diagnostic performance of both imaging techniques in detecting pulmonary tuberculosis. While both CXR and HRCT help identify lung lesions, HRCT demonstrates greater accuracy in early diagnosis and in the detailed detection of parenchymal disease activity.

INTRODUCTION

Pakistan has the world's fifth-highest tuberculosis (TB) prevalence, fourth-highest multi-drug resistant TB (MDR-TB) prevalence, and has 61% of the TB cases in the WHO Eastern Mediter- ranean Region[1]. TB was declared a public health emergency in Pakistan in 2001 and the National

Treatment Program (NTP) initiative was relaunched with an expanded Directly Observed Therapy Short-course (DOTS) program[2]. According to the World Health Organization (WHO) estimates, the nation has over 500 000 incident TB infections per year, with a rising number of drug-resistant cases[3]. This study sought to describe and compare the frequency of key radiologic features of subclinical PTB on chest radiograph (CXR) versus computed tomographic scan (CT), and to interpret the clinical and public health relevance of the differences[4]. Cough and expectoration were significantly frequent in inactive group whereas chest pain was detected higher in active patients. Sensitivity, specificity, positive predictive value, negative predictive value and diagnostic accuracy of HRCT in detecting disease

activity were 88, 88, 92, 83 and 88%, respectively[5]. Computed tomography (CT) is an imaging methodology that uses x-rays to generate detailed pictures or scans, of specific areas of body for diagnosis and therapy[6]. Each image taken in CT procedure is called slice which shows the organs, tissue or bones along a plane[7]. For comparison of radiation exposure levels from different sources, the concept of effective dose equivalent was developed, which is used to assess an individual's risk of developing malignancy[8, 9]. It was the first method that non-invasively accessed inside images of the body[10]. With minimal spatial distance (1 to 1.5 mm) ,the fast imaging and improved image quality, increased the use of HRCT in diagnosis of pulmonary abnormalities[11].

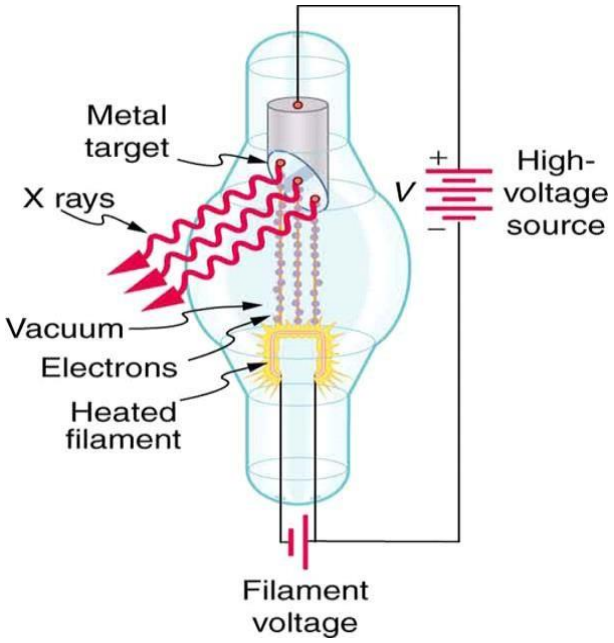


Figure 1.1 high voltage in a vacuum tube, accelerates the thermal electrons[8].

The intensity of the transmitted beam is recorded like a translation function of of the position parameter The transmitted intensity is given by Lambert's law given by the following expression[12, 13].

$$I(x,y)=I0\exp(-\int_{path}\mu(x,y)ds \quad \text{Eqn. (1)}$$

Where I_0 is the incident beam intensity and $\mu(x, y) = f(x,y)$ is the 2D function to rebuild. A new square and rotational coordinates system (t, s) is defined to express the detection system rotatable in comparison to the fixed object coordinates system (or vice versa, if the object is rotating and the detection system is fixed). In the transformation from the system (x, y) to the system (t, s), t is given by

$$t=x.\cos(\theta)+y.\sin(\theta) \quad \text{Eqn. (2)}$$

Material and Method

During my work, we used Toshiba CT scanner system of 64 slices which is installed at radiology department of Bahawalpur Victoria Hospital. This system was introduced in 2004 in the market. Aquilion-64 has 64-row quantum detector and 3-D cone beam algorithms. It has been recognized in the world as true volumetric 64-slice CT scanner. 64 anatomical images per rotation are created by this scanner and provides very thin slice of the organ to be study by physicians. Whole process takes less than 15 seconds. 64-slice CT scanner gives high resolution images and low contrast resolution. It ensures high speed scans with the help of quantum detectors.

HRCT Scan protocols

HRCT can be performed in during both, inspiration and expiration. Slice width is 0.625 to 2 in thickness. Reconstruction algorithm is of high-spatial-frequency for evaluating the lung parenchyma and airways. Field of view and hence size of each pixel is minimum[6]. Gantry rotation time is < 1 second. This fast speed is required to reduce motion artifacts. Data acquisition from axial or incremental HRCT in which axial images of lungs is obtained at 1 to 2 cm increments. 100 kVp and current of 20-40 mAs is used, but for younger patient even low dose is recommended. Variation in mA can reduce the dose. 4. 2 channels detector arrangement is selected on MDCT for axial HRCT. Table speed when needed for single breath acquisition. Radiation dose for chest radiograph is 0.1 mSv [14].

HRCT effective Dose

The HRCT effective dose 0.98 mSv is less then CT scan dose which is 6.5 mSv[6], but HRCT dose is greater than CXR (0.085 mSv)[15].

RESULTS AND DISCUSSION

Statistical Analysis: In total, 20 patients have been imaged and analysed. HRCT demonstrated significantly higher sensitivity than chest radiography in detecting patchy consolidations (70% vs 40%, p = 0.02), air bronchograms (50% vs 0%, p = 0.001), and mediastinal lymphadenopathy (45% vs 15%, p = 0.03). Upper-lobe involvement was the most frequent pattern (75%). Moderate agreement between the two modalities was observed (κ = 0.41).

Table 1: Comparison of CXR vs HRCT Sensitivity

Lesion	CXR (%)	HRCT (%)	p-value
Consolidation	40%	70%	0.02
Air bronchograms	0%	50%	0.001
Lymphadenopathy	15%	45%	0.03

IER
Institute for Excellence in Education & Research

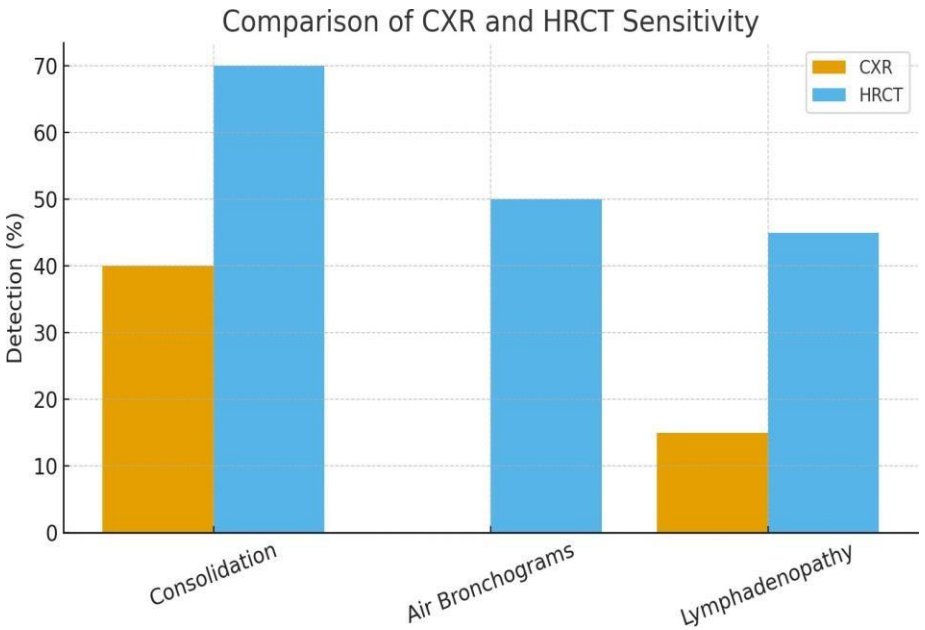


Figure 3.1: Comparison of CXR and High Resolution Computed Tomography

Figure 3.2 shows severe bronchiectasis with marked peri-bronchial thickening and mucus plugging, predominantly in the right middle lobe. These HRCT findings indicate advanced airway inflammation and obstruction, suggesting chronic disease progression and impaired mucociliary clearance.



Fig. 3.2 (a) CT scout film (b) HRCT demonstrates severe bronchiectasis, peribronchial thickening, and mucus plugs, especially in the right middle lobe.

Figure 3.3 demonstrates radiological findings of the chest X-ray with pleural effusion and reduced lung volume. The HRCT scan reveals organized pleural effusions along with irregular pleural thickening on both sides, leading to loss of lung volume and tenting of the pleura.

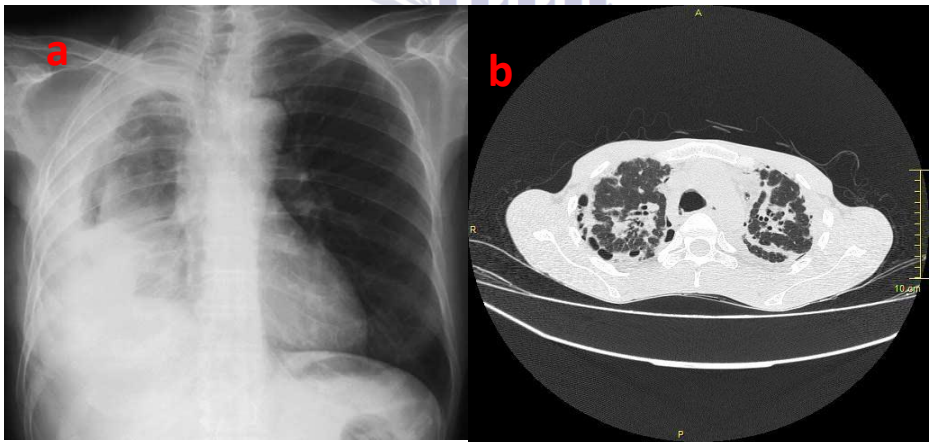


Figure 3.3 (a)Pleural effusion is shown on chest plain film. (b) HRCT shows organized pleural effusions.

Figure 3.4 shows the CT scout film shows reduced lung aeration on the right side. HRCT reveals mild pleural thickening with linear sequelae and loss of lung volume. A small right-sided pleural effusion is also noted. These findings suggest chronic inflammatory changes in the right lung. HRCT scan axial slices reveals loss of lung volume on right side along with pleural effusion on right side of the lung.

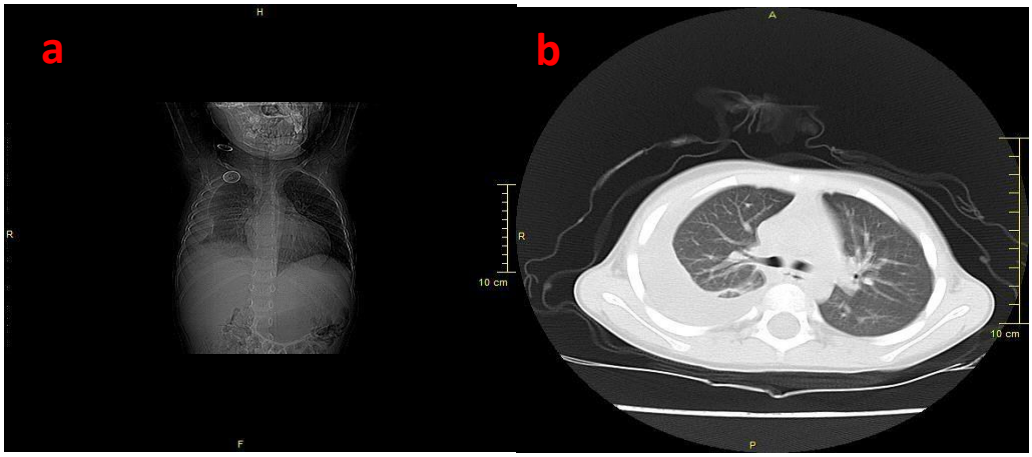


Fig. 3.4(a) CT scout film (b) HRCT sequel linear density with mild pleural thickening.

Figure 3.5 shows the chest X-ray shows patchy consolidation in the right middle lobe with ill-defined borders and visible air bronchograms. HRCT confirms involvement of the same region, demonstrating wall thickening of the anterior segmental bronchus. These findings indicate localized airway inflammation with segmental consolidation.

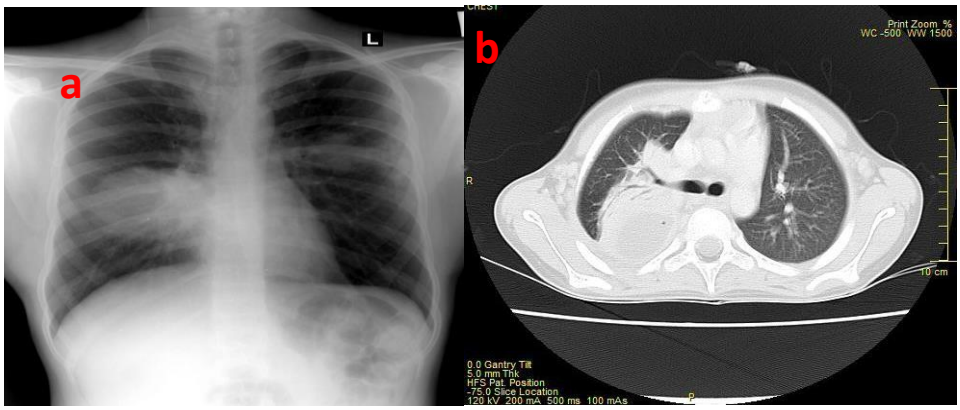


Fig. 3.5(a) Chest plain film shows a patchy consolidation in the right middle lobe(b) HRCT shows wall thickening of the anterior segmental bronchus of the right middle lobe.

Figure 3.6 CT scout film shows diffusely abnormal lung fields suggesting chronic structural changes. HRCT demonstrates marked peri bronchial thickening with multiple areas of air trapping and cystic changes. These findings are consistent with chronic inflammatory lung disease and may represent features of cystic fibrosis–related airway damage.

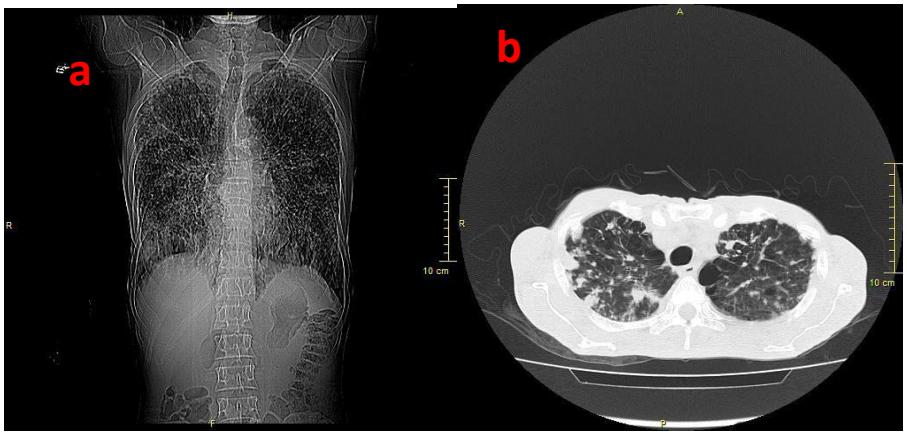


Fig. 3.6(a) CT scout film (b)HRCT. There are peri bronchial thickening and areas of air trapping with cystic fibrosis.

Figure 3.7 shows the CT scout film shows reduced aeration in the right upper lung zone. HRCT demonstrates mild bronchiectasis with peribronchial thickening in the right upper lobe. There is also subsegmental collapse and consolidation in the same region. These findings indicate localized chronic airway inflammation and volume loss.

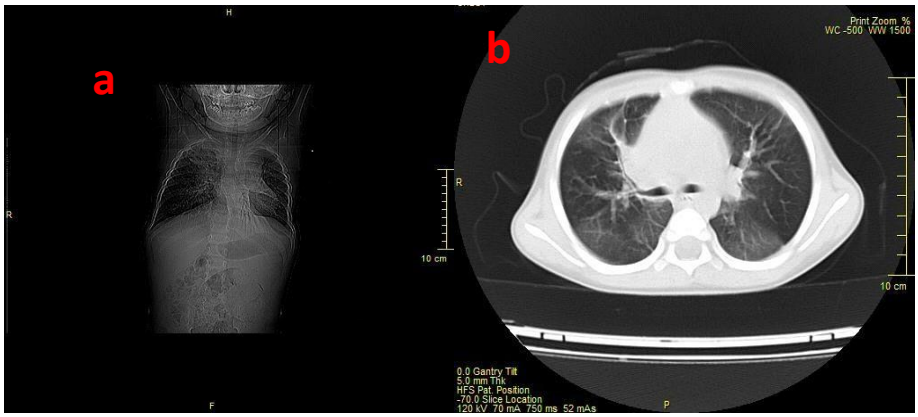


Fig. 3.7(a) CT scout film (b) HRCT sequel linear density with mild bronchiectasis and peri- bronchial thickening in the right upper lob.

Figure 3.8 (a)Chest plain film evidence of significant volume loss in the left upper lobe, along with hilar retraction, cavitation and an “apical cap”. There is also calcified mediastinal and hilar adenopathy (b)HRCT cluster of enlarged homogeneous lymph nodes in the mediastinum is detected.

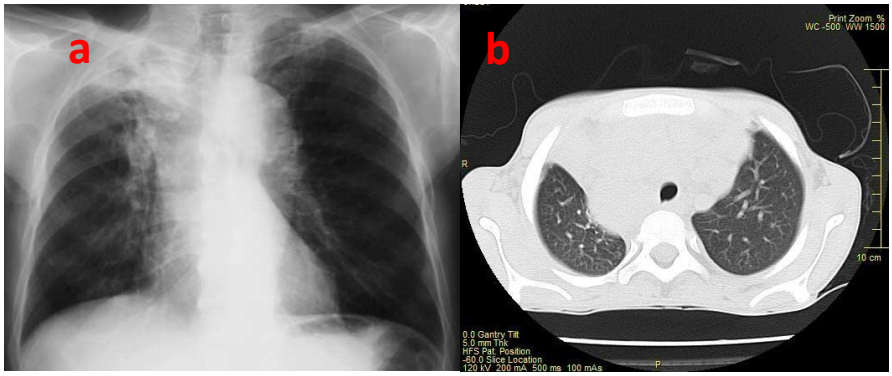


Fig. 3.8 (a)Chest plain (b)HRCT cluster of enlarged homogeneous lymph nodes in the mediastinum is detected.

Figure 3.9 demonstrate the CT scout film shows the overall thoracic outline and lung field alignment. HRCT images reveal clearly defined parenchymal abnormalities. These findings help better characterize the suspicious lesions and support the underlying diagnosis.

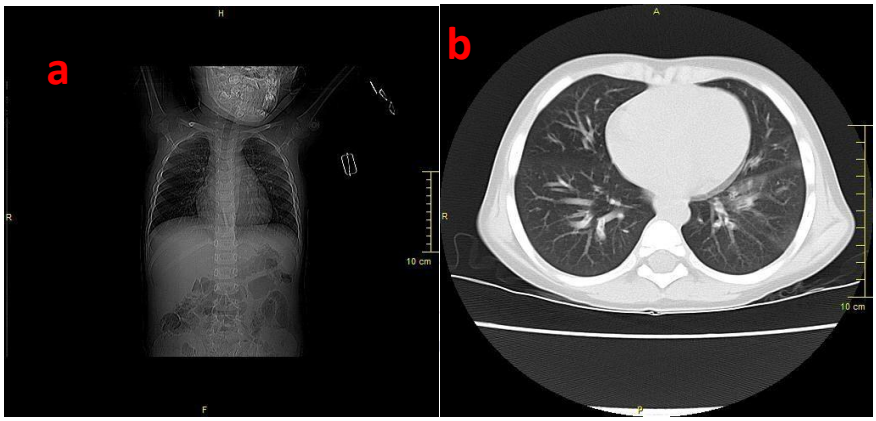


Fig. 3.9(a) CT scout film and (b) High resolution computed tomography.

Figure 3.10 The CT scout film provides a general overview of the thoracic cavity and lung fields. HRCT shows patchy consolidation in the right upper lobe with ill-defined margins. The presence of air bronchograms suggests active parenchymal involvement consistent with infective pathology.

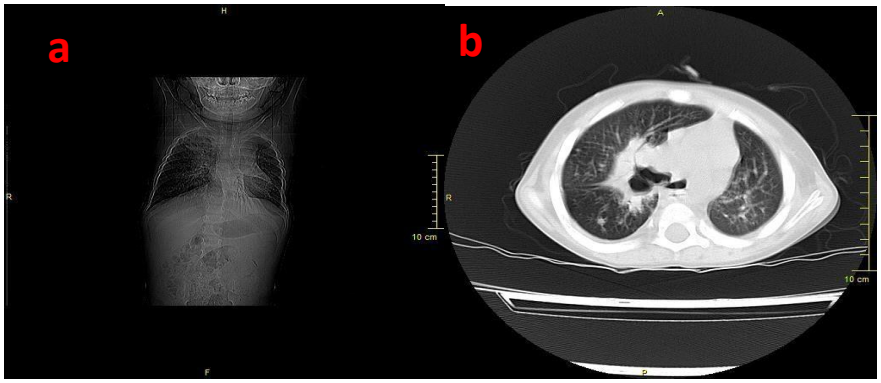


Fig. 3.10(a) CT scout film (b) HRCT patchy consolidation in the right upper lobe with ill-defined borders and air bronchograms.

4. Conclusion

High-resolution computed tomography (HRCT) is more sensitive than chest X-ray (CXR) in the depiction of parenchymal abnormalities. High-resolution computed tomography (HRCT) has been proven to be the best in studying the lesions in different stages and diagnose the pathologies in early phases often before it is apparent clinically. Clinical evaluation is the first step in diagnosis of pulmonary pathologies. Chest Radiography and HRCT examination should be regarded as
integral components of the investigation protocol in patients with various pulmonary parenchymal diseases; as these confirm the clinical suspicion and provide direct evidence of the affected portion. Moreover, HRCT helps to evaluate different phases and progression of disease in relation to prognosis and therapy.

REFERENCES

Braham, C.A., P.J. White, and N. Arinaminpathy, *Management of tuberculosis by healthcare practitioners in Pakistan: A systematic review.* PLoS One, 2018. **13**(6): p. e0199413.

Tahseen, S., et al., *Extrapulmonary tuberculosis in Pakistan- A nation-wide multicenter retrospective study.* PLoS One, 2020. **15**(4): p. e0232134.

Awan, H.A., et al., *Tuberculosis amidst COVID-19 in Pakistan: a massive threat of overlapping crises for the fragile healthcare systems.* 2022. **150**: p. e41.

Lau, A., et al., *A comparison of the chest radiographic and computed tomographic features of subclinical pulmonary tuberculosis.* Sci Rep, 2022. **12**(1): p. 16567.

Ahmed, N., S. Hamid, and M.A. Memon, *Relationship Of Prior Pulmonary Tuberculosis With The Occurrence Of Covid-19 Pneumonia: Review Of 500 Plus HRCT Chest Scans From Two Different Centres Of Sindh, Pakistan.* J Ayub Med Coll Abbottabad, 2021. **33**(3): p. 368-375.

Huda, W., *Radiation doses and risks in chest computed tomography examinations.* Proc Am Thorac Soc, 2007. **4**(4): p. 316-20.

Ors, F., et al., *High-resolution CT findings in patients with pulmonary tuberculosis: correlation with the degree of smear positivity.* J Thorac Imaging, 2007. **22**(2): p. 154-9.

Diederich, S. and H. Lenzen, *Radiation exposure associated with imaging of the chest: comparison of different radiographic and computed tomography techniques.* Cancer, 2000. **89**(11 Suppl): p. 2457-60.

Turkar, A. and A. Babalik, *Comparison of Computed Tomography Findings of Tuberculosis and Non-Tuberculous Mycobacterial Lung Infections.* 2025. **18**: p. 5703-5710.

Chang, G.C., et al., *Low-dose CT screening among never-smokers with or without a family history of lung cancer in Taiwan: a prospective cohort study.* Lancet Respir Med, 2024. **12**(2): p. 141- 152.

Jabeen, C., et al., *A retrospective analysis of tuberculosis in livestock farmers in Lahore district, Pakistan.* J Infect Dev Ctries, 2024. **18**(8): p. 1249-1257.

Kharfi, F., *Mathematics and Physics of Computed Tomography (CT): Demonstrations and Practical Examples*, in *Imaging and Radioanalytical Techniques in Interdisciplinary Research - Fundamentals and Cutting Edge Applications*, F. Kharfi, Editor. 2013, IntechOpen: London.

Martin, S.S., et al., *Impact of noise-optimized virtual monoenergetic dual-energy computed tomography on image quality in patients with renal cell carcinoma.* European Journal of Radiology, 2017. **97**: p. 1-7.

Venkatesh, R., et al., *Acute macular neuroretinopathy with coexistent central retinal vein occlusion as the presenting feature in intraocular tuberculosis.* J Ophthalmic Inflamm Infect, 2020. **10**(1): p. 10.

van der Bruggen-Bogaarts, B.A., et al., *Radiation exposure in standard and high-resolution chest CT scans.* Chest, 1995. **107**(1): p. 113-5.